Kinetics and Polymer Microstructure of the Seeded Semibatch Emulsion Copolymerization of *n*-Butyl Acrylate and Styrene

Christophe Plessis,[†] Gurutze Arzamendi,[‡] Jose R. Leiza,[†] Harold A. S. Schoonbrood,[§,||] Dominique Charmot,[§,⊥] and José M. Asua*[,†]

Institute for Polymer Materials "POLYMAT" and Grupo de Ingeniería Química, Departamento de Química Aplicada, Facultad de Ciencias Químicas, The University of the Basque Country, Apdo. 1072, E−20080 Donostia-San Sebastián, Spain; Departamento de Química Aplicada, Universidad Pública de Navarra, E−31006 Pamplona, Spain; and Rhodia, Centre de Recherches d'Aubervilliers, 52 rue de la Haie Coq, F-93308 Aubervilliers Cedex, France

Received November 29, 2000; Revised Manuscript Received April 14, 2001

ABSTRACT: The seeded semibatch emulsion polymerization of *n*-butyl acrylate, *n*-BA, with varying amounts of styrene as comonomer was investigated using potassium persulfate as initiator at 75 °C. The kinetics, the gel fraction, the molecular weight distribution, MWD, and the level of branches were determined. It was observed that the instantaneous conversion, the fraction of gel, the average molecular weights, and the level of branches were affected by the amount of styrene in the recipe. In particular, the fraction of gel decreased from 55% to almosnt nil and the level of branches decreased from 14 to 5 branches per 1000 carbons of the backbone when the amount of styrene increased from 0 to 10%. These results have technological implications because the amount of gel and the level of branches can be controlled; this is something that was not possible when initiator concentration or monomer feed rates were used as control variables. A mathematical model for predicting the kinetics, the fraction of gel, the level of branches and the MWD was used to analyze the effect of styrene on the seeded semibatch emulsion polymerization of *n*-BA. In addition, it is shown that the adhesive properties of these latexes can be modified by adding small amounts of styrene.

Introduction

Most commercial latexes are copolymers formed by the simultaneous copolymerization of two or more monomers. Copolymerization processes are very relevant to the industrial environment because they allow the preparation of polymers with a wide range of properties such as impact and solvent resistances, compatibility, and elasticity.[1] The final latex properties are determined by factors such as the copolymer composition, sequence distribution, molecular weight distribution (MWD), frequency of branches or cross-link points, and morphology of the particles. To control these properties, different operational variables can be used (temperature, initiator, chain transfer agent (CTA), and comonomer) as well as different reactors (batch, semibatch, and continuous) and also different control strategies.[2]

Numerous papers can be found in the literature[3−12] dealing with the emulsion copolymerization of *n*-butyl acrylate (*n*-BA) and styrene (S). Because of the different nature of these monomers, a wide range of materials with interesting mechanical properties can be obtained varying the comonomer ratio. Cruz et al.[6] investigated the kinetics of the emulsion copolymerization of *n*-BA/S. They found that the comonomer compositions and the reaction pathways affect the particle morphology, the molecular weight and colloidal properties. Their kinetic study showed that the reactivity ratios ($r_S = 0.75$, $r_{BA} = 0.20$) determined in batch emulsion polymerization at low conversion are close to those obtained in bulk or solution polymerization.[8] Recent works[9,10] showed that the effective reactivity ratios could be a function of instantaneous conversion, because the viscosity of the reaction media affected the monomer diffusion to macroradicals.

Chrastova et al.[7,11] studied the influence of the initiator type on kinetics, molecular weights and particle size in batch emulsion copolymerization of *n*-BA and S in a wide range of comonomer compositions (*n*-BA/S: 10/90 to 90/10). Using redox initiator systems of different water solubilities, they found that the larger the amount of styrene the smaller the molecular weights. However, the molecular weights were very high (within 2×10^6 to 15×10^6). Furthermore, they did not report any presence of gel in their latexes. Recently, Yang et al.[12] used a factorial design to investigate the emulsion copolymerization of *n*-BA/S finding that the comonomer ratio, reaction temperature and surfactant concentration were the key variables affecting the polymerization rate and MWD. They also observed that under batch conditions, the molecular weights decreased with increasing styrene concentration, and for compositions in the range *n*-BA/S = 10/90−90/10 and at reaction temperatures between 60 and 70 °C, no gel was reported.

Charmot[13] reported that the homopolymerization of *n*-BA yielded a gel in batch reaction, but this amount was virtually zero when, under the same conditions, butyl methacrylate was used instead. Charmot[13] argued that BMA does not suffer transfer to polymer reaction because no tertiary protons were present in the poly-BMA chain.

Plessis et al.[14−17] have also reported that the seeded semibatch emulsion polymerization of *n*-BA produced

* To whom correspondence should be addressed. E-mail: qppasgoj@sq.ehu.es.
[†] University of the Basque Country.
[‡] Universidad Pública de Navarra.
[§] Rhodia, Centre de Recherches d'Aubervilliers.
[||] Current address: Wacker Chemicals Australia, Pty. Ltd., Suite 3, 11 Leicester Avenue, Glen Waverley, 3150 VIC Australia.
[⊥] Current address: SYMYX Technologies, Inc., 3100 Central Expressway, Santa Clara, CA 95051.

10.1021/ma0020382 CCC: $20.00
Published on Web 06/22/2001

Table 1. Seed Formulation

n-butyl acrylate (g)	250
water (g)	1000
SLS (g)	5.0
$NaHCO_3$ (g)	1.25
$K_2S_2O_8$ (g)	1.25

Table 2. List of Semicontinuous Experiments Carried out with Different Amounts of Styrene

	amount of styrene (wt %)	feeding time (h)
	Effect of Comonomer Composition	
run 1	0	3
run 2	1	3
run 3	2.5	3
run 4	5	3
run 5	10	3
	Effect of Feeding Time	
run 6	5	6
run 7	10	6

gel and that this was mainly due to intermolecular transfer to polymer plus termination by combination. They have also shown (experimentally and validated by a mathematical a model) that the amount of gel formed in the process was not significantly affected by varying the initiator concentration and the monomer feed rate, but it was by the addition of chain transfer agent, CTA. The addition of CTA also strongly reduces the molecular weights of the sol and hence the mechanical properties of the adhesives were considerably damaged.

This work reports on the effect that small amounts of styrene (lower than 10 wt %) have on the kinetics and specifically on the structural properties of the latexes (gel, MWD of the sol and branching level) which definitely influence the properties of the adhesives which are sought from this type of latexes.

Experimental Section

Materials. *n*-Butyl acrylate, styrene, and acrylic acid (Atochem), sodium lauryl sulfate, (SLS, Merck), sodium hydrogen carbonate (Panreac), and potassium persulfate (Fluka) were all used as received. SLS was used to prepare the seed, and a mixed emulsifier system (a mixture of ethoxilated anionic and nonionic surfactants provided by Rhodia) was used for the semicontinuous experiments. The composition of this system, which will be called surfactant A, cannot be disclosed due to proprietary reasons. All polymerizations were carried out using doubly deionized water.

Preparation of Latexes. All reactions were seeded. The poly(*n*-BA) seed was prepared batchwise following the formulation shown in Table 1 in a 2 L reactor at 65 °C and kept overnight at 90 °C in order to decompose the unreacted initiator. Two series of experiments were carried out in semicontinuous conditions as summarized in Table 2. Both the comonomer composition (equal or lower than 10 wt % in styrene) and the monomer feeding time were varied. The seeded semicontinuous emulsion copolymerizations were carried out at 75 °C in a 1 L glass reactor fitted with a reflux condenser, a sampling device, a nitrogen inlet, two feed inlet tubes, and a stainless steel agitator comprising an anchor at the bottom and three equally spaced 2-blade impellers along the shaft (agitation speed: 200 rpm).

Table 3 shows the formulation used. The experimental procedure was as follows: the seed ($d_p = 97$ nm; solids content = 20.5 wt %; gel content = 10 wt %; branching level = 0.9% and $\bar{M}_w = 2.2 \times 10^6$ g/mol) and a part of surfactant A, initiator, and water were initially charged into the reactor. The rest was fed divided in two streams having both the same total feeding time: one was a preemulsion containing monomer and the other the initiator in aqueous solution.

Characterization. Samples withdrawn from the reactor during the polymerization were analyzed gravimetrically to determine the instantaneous conversion (based upon the total monomer fed until the sampling time). The cumulative copolymer composition was determined by gas chromatography (Shimadzu GC-14A using a column 25QC5/BP5 1.0, Scientific Glass Engineering Inc.) and by ^{1}H NMR spectroscopy. For NMR, copolymer samples were examined as a 5 wt % solution in deuterated chloroform, $CDCl_3$; the spectra were recorded at 20 °C using a Varian XLS spectrometer (300 MHz). The copolymer composition was calculated by comparing the integrated intensities of the resonance signals due to the phenyl protons of S and that of the methylene group closest to the oxygen in the ester group of *n*-BA.

Table 3. Formulation Used for the Seeded Semicontinuous Emulsion Polymerizations

	initial charge	stream 1	stream 2
seed (g)	100		
water (g)	17.5	20	255
surfactant A (g)	1.25		2.5
n-butyl acrylate (g)			variable
styrene (g)			variable
acrylic acid (g)			4.6
$K_2S_2O_8$ (g)	0.375	0.375	

Particle size was measured by dynamic light scattering spectroscopy, DLS (Coulter N4-Plus), and by capillary hydrodynamic fractionation, CHDF (Matec Applied Sciences, model 2000). The value obtained by DLS was used for the calculation of the number of polymer particles and the CHDF measurements were used to check for secondary nucleations.

The molecular weight distribution and the weight-average molecular weights of the copolymer were determined by size exclusion chromatography, SEC, at 40 °C. The SEC instrument consists of a pump (Waters model 510), three columns (Styragel of porosity 10^2, 10^4, and 10^6 Å), and a dual detector system formed by a differential refractometer and a viscometer (Viscotek model 250). Samples were diluted in tetrahydrofuran (THF) at an approximate concentration of 0.3% (w/v). The flow rate for THF was 1 mL min^{-1}. Polystyrene standards were used to calibrate the apparatus. On the basis of this calibration, the product of intrinsic viscosity by the molecular weight, $[\eta]M$, is known as a function of the retention time. The intrinsic viscosity is measured directly by the viscometer and this allows us to determine the molecular weight of the sample without using the Mark−Houwink constants for *n*-BA.

A modified Cohen Addad process[18] was used to measure the gel content of the polymer film. The process consisted in a continuous extraction with THF under reflux in a 1 L glass reactor. The amount of gel, G, can be calculated using eq 1,

$$G = \frac{w_g}{w_p} \tag{1}$$

where w_g and w_p are the weights of insoluble fraction and the whole sample, respectively.

To quantify the level of branching of the copolymer, solid state ^{13}C NMR analysis were carried out. Final latexes were dried under vacuum at room temperature, and the dry polymer sample was slightly swollen in $CDCl_3$ before being analyzed. Solid state ^{13}C NMR spectra were obtained at 60 °C using a Bruker Avance DSX300. Spectra runs were collected by using a 7 mm CP-MAS probe, a pulse interval of 8 s and a spin of 3000 Hz. At least 25000 acquisitions were collected for each spectrum. A typical spectrum of the latexes produced during this work is presented in Figure 1. Peak assignments were used as previously determined in the literature for homopolymers of *n*-BA[14,19,20] and styrene[21] and are presented in Table 4. The percentage of branches was calculated as reported in the literature[14,19] using eq 2 where A_i is the area of peak i in

$$\% \text{ branches} = \frac{A_I}{A_I + \frac{A_{F-H}}{2}} \times 100 \tag{2}$$

Figure 1 and Table 4.

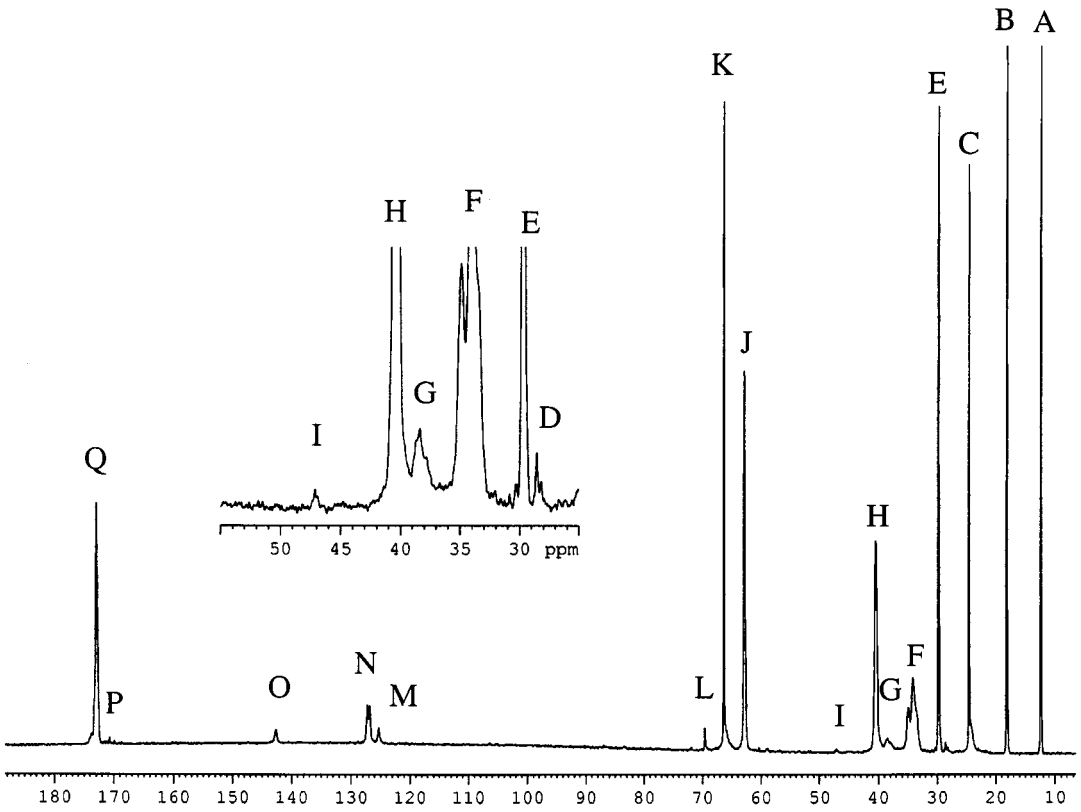

Figure 1. Solid state ^{13}C NMR spectrum of the copolymer *n*-BA/S. Peaks are labeled as in refs 15 and 19.

Table 4. Peak Assignments for the ^{13}C NMR Spectrum of the *n*-BA/S Copolymers[14,19−21]

peak	chem shifts δ_c/ppm	assignment
A	12.8	BA CH_3
B	18.1	BA 3-CH_2
C	24.3	THF
D	28.1−29.0	end group $-CH_2CH_2COOBu$
E	30.1	BA2−CH_2
F	32.5−36.0	BA−BA CH_2
G	37.3−39.7	branch CH_2 and CH
H	40.4	BA CH
I	47.2	branch Cq
J	62.4	BA 1-CH_2
K	66.5	THF
L	69.5	surfactant
M	125.5	S $CH_{(4)}$
N	127.4	S $CH_{(2-3)}$
O	144.5	S $C_{(1)}$
P	174.8	BA C=O
Q	175.4	terminal or branch C=O

Adhesive properties such as tack, shear, and peel resistances of the *n*-BA/S copolymer latexes were measured to study the effect of the molecular weight distribution and the fraction of gel on adhesion properties. The backing used in this work was an electrostatically discharge-treated poly(propylene) film 29 μm thick (Polygal Spain). The latexes, with a solids content of about 41 wt % and a viscosity of about 1−2 cP, were applied on the poly(propylene) film by means of a metallic applicator, ensuring the formation of a continuous 90 μm coat, and then introduced for 20 min to an oven at 50 °C. The adhesive tape was then cooled for 20 min at room temperature, and after this period, the different tests were carried out.

In this work, the rolling ball tack test was used to measure the tack of the polymer films. In this procedure, a 11 mm diameter stainless steel ball is rolled down on an inclined track to come into at the bottom with the horizontal, upward-facing adhesive.[22] The distance the ball travels out along the tape is taken as the measure of tack. Ball rollout distance gives an inverse scale of tack: the greater the distance, the less tacky the film.

To determine the resistance to shear, the method used here consists of applying, under pressure, a standard area of tape (25 mm × 25 mm) to a panel 2° from the vertical (the purpose of the small inclination from vertical being to ensure that the tape will experience no peeling action, only shear) covered with kraft paper and applying a standard mass (1000 g) until failure.[22] The time (in seconds) between the application of the load and the separation of the tape from the panel is the measurement of shear.

The 180° test was used to determine the resistance to peel force of PSA tapes. A 20 mm wide tape is applied to a standard metallic panel, using definite pressure (a 2 kg roller) to make contact; 10 min later, the free end of the tape is doubled back at an angle of 180° and clamped to the upper jaw of an Instron tensile tester. The upper jaw is then operated at the set speed of 300 mm/min. The values obtained while the first 25 mm of tape is mechanically peeled are disregarded, and the adhesion value considered is the average pull value obtained during peeling the next 50 mm. It is expressed in N/100 mm.[22] Fifteen replicated measurements were carried out for the tack and resistance to shear tests, and the average and standard deviation were calculated. For the resistance to peel test, five measurements were carried out, and the average value and standard deviation were also calculated.

Mathematical Model

A mathematical model developed in a previous work for the homopolymerization of *n*-BA[16] was adapted for the *n*-BA/S emulsion copolymerization. The mathematical model uses the numerical fractionation technique[23−25] and accounts for radical compartmentalization by means of the partial distinction concept of radicals.[26]

For the sake of brevity in what follows, only the distinctive kinetic aspects of the polymerization of *n*-BA/S will be described and discussed. The following kinetic events were accounted for in the mathematical model: (i) initiation of polymer chains from radicals entering into the particles or produced by a chain

Scheme 1

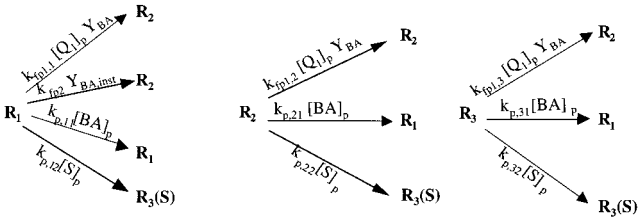

transfer reaction; (ii) linear propagation; (iii) chain transfer to monomer; (iv) intermolecular chain transfer to polymer; (v) intramolecular chain transfer to polymer or backbiting; and (vi) termination by combination. The material and population balances are given in Appendices I and II. A complete description of the mathematical model can be found in ref 16.

Plessis et al.[14−17] reported that, in the polymerization of *n*-BA, intramolecular chain transfer to polymer (backbiting) was the predominant chain transfer to polymer reaction. This process produced a decrease of the overall polymerization rate due to the formation of a tertiary radical with an extremely low reactivity.[14] Therefore, in the copolymerization of *n*-BA/S three types of radicals should be considered: (i) R_1, the secondary radical with the ultimate unit of type *n*-BA; (ii) R_2, the tertiary radical resulting from chain transfer to polymer (both intramolecular and intermolecular); (iii) $R_3(S)$, the radical with the ultimate unit of type S. The kinetic scheme shown in Scheme 1 was considered for the different radicals, where $k_{fp1,i}$ is the intermolecular chain transfer to polymer rate constant of a radical with an ultimate unit of type i; $[Q_1]_p$ the concentration of polymer in the polymerization loci (polymer particles); Y_{BA} the cumulative copolymer composition referred to *n*-BA; k_{fp2} the intramolecular chain transfer to polymer rate constant; $k_{p,ij}$ the propagation rate constant of radicals R_i with monomer *j*; $Y_{BA,inst}$ the instantaneous copolymer composition referred to *n*-BA, and $[M]_p$ the concentration of the monomer in the polymer particles.

In this work, it was considered that the intermolecular transfer to polymer of radicals R_1 is larger than that of radicals R_2, namely that tertiary radicals are also less reactive for H abstraction. In our previous works on homopolymerization,[14,17] it was considered that $k_{fp1,1} = k_{fp1,2}$. Nevertheless model predictions using the new parameters do not significantly differ from those in refs 14 and 17 because the effective intermolecular chain transfer to polymer rate constant of *n*-BA $\bar{k}_{fp1} = k_{p,1.1}P_1 + k_{fp1.2}P_2$ is roughly the same. Also it is assumed that the tertiary radical reacts faster with styrene than with *n*-butyl acrylate as follows: $k_{p,22.1}/k_{p,22} = k_{p,11}/k_{p,12} = r_{BA}$. In addition, only radicals R_1 can undergo backbiting. Average kinetic coefficients were used in the copolymerization model.

Propagation.

$$\bar{k}_p[M] = \sum_{i=1}^{3}\sum_{j=1}^{2} k_{p,ij}P_i[j]_p \tag{3}$$

where P_i is the probability of finding a radical with ultimate unit of type *i*.[27]

Chain Transfer to Monomer.

$$\bar{k}_{fm}[M] = \sum_{i=1}^{3}\sum_{j=1}^{2} k_{fmij}P_i[j]_p \tag{4}$$

where $k_{fm,ij}$ is the chain transfer to monomer rate constant of a radical of type *i* with a monomer of type *j*.

Termination by Combination. In the absence of gel effect, the average termination rate constant is

$$\bar{k}_{t,o} = k_{t,11}P_1^{\,2} + k_{t,22}P_2^{\,2} + k_{t,33}P_3^{\,2} + 2k_{t,12}P_1P_2 + 2k_{t,13}P_1P_3 + 2k_{t,23}P_2P_3 \tag{5}$$

with

$$k_{t,ij} = (k_{t,ii}k_{t,jj})^{1/2} \quad \text{and} \quad k_{t,ij} = k_{t,ji} \tag{6}$$

where $k_{t,ij}$ is the rate constant for termination by combination between radicals of type *i* (R_i) and type *j* (R_j), respectively. It was considered that the radicals R_1 and R_2 have the same termination rate, namely, that $k_{t11} = k_{t22} = k_{t12} = k_{t21}$. When the termination reaction in the polymer particles becomes diffusion-controlled, the termination rate constant decreases by several orders of magnitude.[28−30] This decrease in the termination rate constant, always causes a significant increase in the rate of the polymerization and can also shift the molecular weight distribution toward higher molecular weights. Under these circumstances, the average termination rate constant becomes

$$\bar{k}_t = \bar{k}_{t,o}g \tag{7}$$

where *g* is given by

$$g = \exp((a_1Y_{BA} + a_2(1 - Y_{BA}))\Phi_p^p) \tag{8}$$

where Φ_p^p is the polymer fraction in the polymer particles and a_1 and a_2 are coefficients.

Intermolecular Chain Transfer to Polymer. The average rate coefficient for intermolecular chain transfer to polymer is

$$\bar{k}_{fp1} = (k_{fp1,1}P_1 + k_{fp1,2}P_2 + k_{fp1,3}P_3) \tag{9}$$

where $k_{fp1,i}$ is the chain transfer rate constant to polymer of a radical of type *i* on *n*-BA polymerized units in the polymer chain. It is considered that only the hydrogen linked to the tertiary carbon of the backbone belonging to *n*-BA polymerized units was able to undergo the transfer reaction; namely that the hydrogen on the tertiary carbon belonging to polymerized styrene was very stable.

Intramolecular Chain Transfer to Polymer (Backbiting). It is considered that only radicals with ultimate unit of type *n*-BA, that is R_1 radicals, were able to produce backbiting. In addition, it is assumed that the probability of having a hydrogen linked to the tertiary carbon of a *n*-BA polymerized unit is equal to the instantaneous copolymer composition referred to *n*-BA. The backbiting rate constant is given by

$$\bar{k}_{fp2} = k_{fp2}P_1 \tag{10}$$

The mathematical model includes numerous parameters. Some of them are available in the literature, but others are not available or the range of parameters reported in the literature is very broad. Table 5 presents the parameter values taken from the literature.

(i) The rate constant for radical entry into the particles varies with the radius of the swollen polymer particle.[31] The exact dependence is a function of the mechanisms for radical entry. Diffusional entry has been reported to be the entry mechanism for several systems including the copolymerization of styrene and

Table 5. Values of Parameters Used for the Model Predictions in Figures 1−9

k_a^* (dm²/mol/s)	4.2×10^{-11} [a]		
k_d (dm² s^{-1})	8.5×10^{-13} [a]		
r_{BA}, r_S	0.2[7]	0.75[7]	
gel effect: a_1, a_2	−2.23[16]	−0.01 [a]	
n_e	50		
n_c	not limited		
	R_1	R_2	R_3(S)
k_p (L/mol/s)	53 460[16]	100[16]	542[34]
k_{to} (L/mol/s)	6.55×10^{6} [16]	6.55×10^{6} [16]	5×10^{8} [35]
C_M	8.85×10^{-5} [37]	8.85×10^{-5} [37]	1.5×10^{-4} [38]
k_{fp1} (L/mol/s)	0.630[a]	0.159[a]	0.005[a]
k_{fp2} (s^{-1})	924[16]		

[a] Estimated in this work.

butyl acrylate.[3] Therefore, this mechanism was considered to be operative in the present case and, hence $k_a = k_a^* r_p$, where k_a^* was the adjustable parameter.

(ii) The desorption rate constant, k_d, also depends on particle size. For sparingly water-soluble monomers in the absence of CTA, Asua et al.[32] predicted that $k_d = k_d^*/r_p^2$, where k_d^* was taken as the adjustable parameter. Note that k_d cannot be larger than the rate of generation of single-unit radicals in the polymer particles.

(iii) $k_{fp1,3}$, intermolecular transfer to polymer (in *n*-BA polymerized monomeric units) of radicals having ultimate unit of type S, R_3 radicals, was taken as adjustable parameter.

(iv) The coefficient a_2 in eq 8 was also estimated.

(v) The intermolecular chain transfer to polymer rate coefficients for radicals R_1, $k_{fp1.1}$, and R_2, $k_{fp1.2}$, were estimated.

The estimation was carried out using the Nelder and Mead algorithm[33] of direct search (DBCPOL subroutine, IMSL library). The following objective function was minimized:

$$J = \left[\sum_N \sum_{n_1(N)} \frac{w_1}{n_1(N)} \left(\frac{X_{\text{inst}_{\text{exp}}} - X_{\text{inst}_{\text{mod}}}}{X_{\text{inst}_{\text{exp}}}} \right)^2 + \sum_N \sum_{n_2(N)} \frac{w_2}{n_2(N)} \left(\frac{B_{\text{exp}} - B_{\text{mod}}}{B_{\text{exp}}} \right)^2 + \sum_N \sum_{n_3(N)} \frac{w_3}{n_3(N)} \left(\frac{\text{Gel}_{\text{exp}} - \text{Gel}_{\text{mod}}}{\text{Gel}_{\text{exp}}} \right)^2 + \sum_N \sum_{n_4(N)} \frac{w_4}{n_4(N)} \left(\frac{\bar{M}_{w_{\text{exp}}} - \bar{M}_{w_{\text{mod}}}}{\bar{M}_{w_{\text{exp}}}} \right)^2 \right] \quad (11)$$

where N is the number of experiments; w_i the weighting factors, and $n_i(N)$ the number of experimental points in each experiment; Z_{exp} and Z_{mod} the experimental and simulated values of the variable Z, namely, instantaneous conversion (X_{inst}), branching level (B), gel content (Gel) and weight-average molecular weight ($\bar{M}_w$). The values of w_i used were as follows: $w_1 = 10^3$; $w_2 = 5 \times 10^5$; $w_3 = 1$; $w_4 = 1$. These values were chosen to cause each of the terms in eq 11 to have a similar value.

Table 5 presents the values of kinetic parameters estimated in this work.

Results and Discussion

Effect of the Comonomer Composition in the Feed. In runs 1−5, the amount of styrene was varied within 0−10 wt % based on the total amount of monomer. The other process variables were kept constant as presented in Table 3. Figure 2 shows the evolution of the model predicted and experimental instantaneous conversions. In this plot, overall conversion was defined as the ratio between the polymerized monomer at the sampling time and the total monomer present in the formulation. It can be seen that the polymerization rate is clearly affected by the amount of styrene used in the feed; the larger the styrene content the lower the instantaneous conversion. This effect was not due to a variation in the total number of polymer particles that was independent of the styrene content in the feed (Figure 3). Figure 2 also shows that the model predicts fairly well the effects of the addition of styrene on kinetics. The model shows that the decrease of the instantaneous conversion was due to the lower propagation rate constant of styrene ($k_{p,S}$) = 542 L/mol/s[34] and $\bar{k}_{p,BA} = (6-7) \times 10^3$ L/mol/s[14] at 75 °C) as well as to a decrease in the average number of radicals per particle when the styrene content increased. Styrene radicals have a higher termination rate than *n*-BA radicals;[35,36] this means that the average termination rate increases with the styrene content.

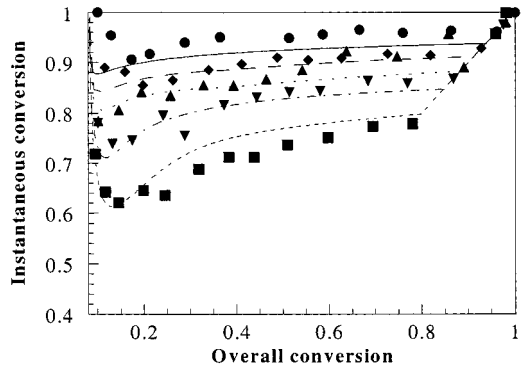

Figure 2. Evolution of the instantaneous conversion for the experiments in which the amount of styrene was varied within 0−10 wt %. Legend: (●, —) 0 wt %; (◆, − −) 1 wt %; (▲, ···) 2.5 wt %; (▼, - -•- -) 5 wt %; and (■, − - − -) 10 wt %. Symbols are experimental data and lines model predictions.

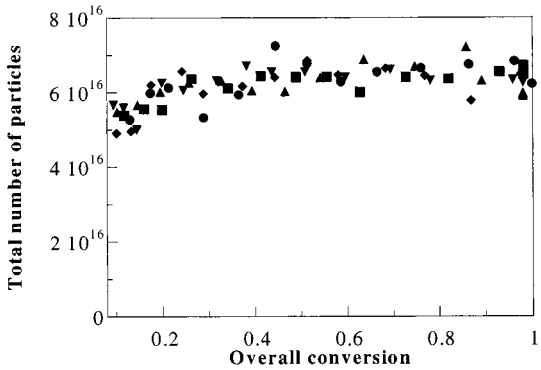

Figure 3. Evolution of the total number of polymer particles when the amount of styrene was varied in the feed (feeding time = 3 h). Legend: (●) 0 wt % (run 1); (◆) 1 wt % (run 2); (▲) 2.5 wt % (run 3); (▼) 5 wt % (run 4) and (■) 10 wt % (run 5).

Figure 4 shows the simulated average number of radicals per particle for runs 1−5. It can be seen that the larger the amount of styrene, the smaller $\bar{n}$. The decrease in $\bar{n}$ is basically due to the larger termination rate constant of styrene, (the effect of chain transfer to monomer and radical desorption being less important).

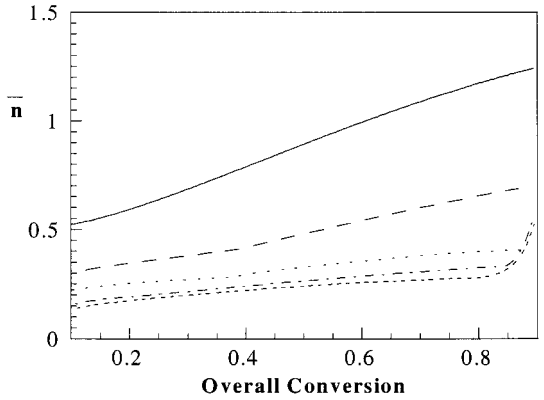

Figure 4. Predicted average number of radicals per particle for runs 1−5. Legend: (—) 0% (run 1); (− −) 1 wt % (run 2); (···) 2.5 wt % (run 3); (- -·- -)−5 wt % (run 4) and, (- -)10 wt % (run 5).

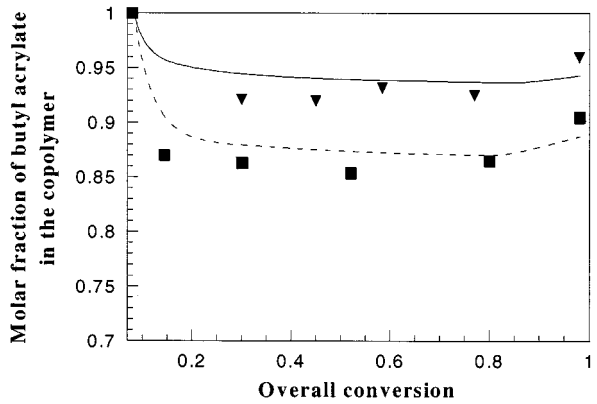

Figure 5. Cumulative copolymer composition referred to *n*-butyl acrylate for runs 4 and 5. Legend: (▼) ^{1}H NMR and (—) model 5 wt % (run 4); (■) ^{1}H NMR and (- -) model 10 wt % (run 5).

Moreover, when the amount of styrene is larger than 1 wt %, $\bar{n}$ remained well below 0.5 during the monomer-feeding period.

Figure 5 shows the experimental and model predicted cumulative copolymer composition for runs 4 and 5. Initially the composition was equal to 1 because the seed was made of poly(*n*-BA). It can be observed that the amount of styrene in the copolymer was slightly larger than the composition of the feed stream. This result agrees well with previous works[3,6,7,9,10] in which it was found that the styrene was more reactive than *n*-BA. In addition, a good agreement was obtained between the theoretical predictions and the experimental data for the cumulative copolymer composition, which basically means that the reactivity ratios considered by the model are correct.

Figure 6 presents the simulated and experimental values of the level of branches for the final latexes. It can be observed that the addition of small amounts of styrene affects the level of branches; the larger the amount of styrene, the smaller the branching frequency. The model shows that the level of branches decreases because: (i) the probability of having a radical of type 1, R_1, decreased when increasing the amount of styrene in the recipe (note that styrene is more reactive than *n*-BA), (ii) the fraction of *n*-BA units in the polymer chain decreased as styrene concentration increased, and (iii) the total amount of unreacted monomer in the particles was considerably increased when adding styrene, and following the rationale of the kinetic scheme

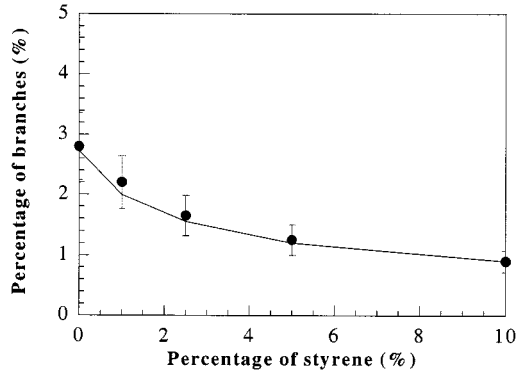

Figure 6. Experimental and predicted level of branches of the final latexes for the experiments with varying amounts of styrene. Legend: (●) ^{13}C NMR and (—) model.

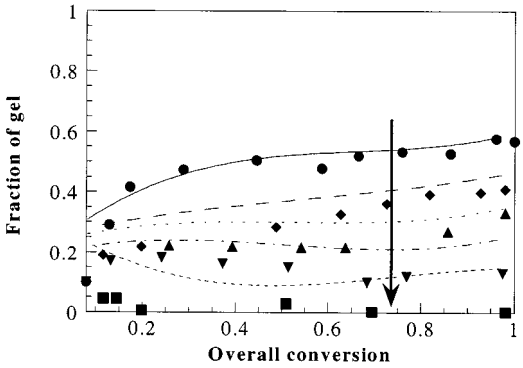

Figure 7. Experimental and predicted gel fractions for experiments with varying amounts of styrene. Legend: (●, —) 0 wt %; (◆, − −) 1 wt %; (▲, ···) 2.5 wt %; (▼, - -·- -) 5 wt %; and (■, - -) 10 wt %. Symbols are experimental data and lines model predictions.

presented above, the level of branches was a function of the concentration of monomer in the polymer particles; namely that the larger the monomer concentration in the polymer particles the smaller the level of branches.

The model also shows that backbiting is the main mechanism leading to the formation of branches. The number of long chain branches, LCB, formed by intermolecular transfer to polymer reaction (k_{fp1}) was 2 orders of magnitude lower than the short chain branches, SCB. This is in agreement with the results reported for the semicontinuous emulsion homopolymerization of *n*-BA.

Figure 7 shows the gel fraction produced in runs 1−5 and the predictions of the mathematical model. Before going into detail on this figure, it is worth taking the time to explain how gel might be formed in a free radical polymerization. The addition of small amounts of cross-linking agents (such as ethylene glycol dimethacrylate) can lead to the production of polymer networks that yield gel. Gel can also be formed by intermolecular chain transfer to polymer coupled with propagation to terminal double bonds or termination by combination. For the emulsion homopolymerization of *n*-BA without the use of any cross-linking agent, it has been demonstrated that the latter mechanism is the one leading to the formation of gel.[14−17,23] In Figure 7, it is shown that the amount of gel produced in a seeded semibatch emulsion copolymerization of *n*-BA/S strongly depends on the amount of styrene used as comonomer. Furthermore, it is shown that 10 wt % of styrene is enough to avoid the formation of gel, which is in agreement with

Table 6. Measurements of Adhesive Properties (Tack, Shear and Peel Resistances) for the Latexes Prepared with 0, 2.5, and 10 wt % of Styrene as Comonomer and with 0.06 and 0.15 wt % of CTA[17]

amount of CTA (wt %)[a]	0	0	0	0.06	0.15
amount of styrene (wt %)[a]	0	2.5	10	0	0
gel fraction (%)	55	32	1	32	1
$\bar{M}_w$	523.000	1.188.000	1.580.000	430.000	340.000
tack (cm)	0.5 ± 0.2	0 ± 0	0.7 ± 0.3	0 ± 0	0 ± 0
shear (s)	40 ± 10	1662 ± 106	1051 ± 117	1820 ± 210	45 ± 12
peel (N/100 mm)	16.9 ± 1.6	26.0 ± 0.6	6.0 ± 1.1	23.4 ± 3.6	11.0 ± 1.1

[a] Weight percentage based on the total monomer weight.

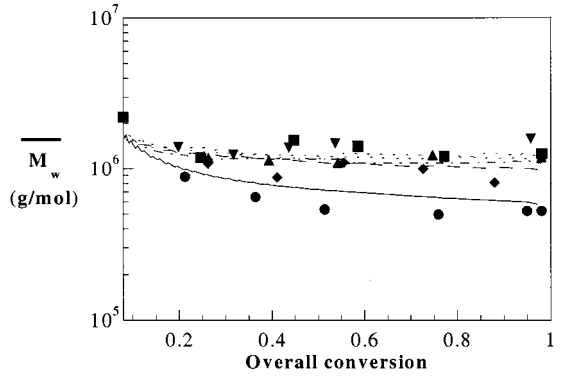

Figure 8. Evolution of the experimental and predicted weight-average molecular weights for experiments with varying amounts of styrene.

previous works on *n*-BA/S.[11,12] Model predictions on gel are in reasonable agreement with the trends observed experimentally when the amount of styrene was increased in the recipe. This means that our model captured well the mechanism leading to gel formation on the copolymerization of *n*-BA/S. Basically, the model shows that the gel decreased with increasing the styrene content because the probability of having secondary butyl acrylate radicals, R_1, decreased, and the styrene radicals, R_3, are less reactive for the intermolecular chain transfer to polymer (see Table 5). In addition, the larger termination rate constant of styrene radicals reduced average number of radicals per particle, which in turn lowered the probability of termination by combination of long radicals.

Figure 8 shows the evolution of the weight-average molecular weights for runs 1−5. The model predicts well the experimental observations; that is by increasing the amount of styrene, the final $\bar{M}_w$ increases and that, within the experiment, the decrease of the $\bar{M}_w$ is less pronounced than for the homopolymerization of *n*-BA. The evolution of $\bar{M}_w$ was largerly due to that of the gel content. Gel formation involves chain transfer to large polymer chains followed by termination by combination. Consequently gel formation results in a decrease of the sol molecular weights: namely, the higher the gel fraction the smaller the sol molecular weights.

It is worth noting that these results do not follow the trend observed in previous publications for the emulsion copolymerization of *n*-BA/S.[8,12] These works reported that as the amount of styrene was increased, the $\bar{M}_w$ decreased. However, these copolymerizations were carried out at styrene concentrations larger than 10 wt %, and under these conditions no gel was formed.

Table 6 presents the adhesives properties of the latexes prepared with 0, 2.5, and 10 wt % of styrene and also the data reported in a previous publication[17] for poly *n*-BA latexes prepared with different amounts of chain transfer agent. As can be seen, all the latexes presented an excellent tack, which is one of the requirements for a pressure sensitive adhesive (PSA). The amount of styrene added had no effect on the tack of these latexes. The main reason is that the sol MWD of these latexes was quite broad and sufficient low molecular weight chains were present to provide tackiness. Resistance to shear and peel were noticeably affected by the addition of styrene. The latex with the highest gel fraction (55% prepared without any styrene in the formulation) shows a weak resistance to shear, likely because the large amount of gel precluded particle interpenetration during film formation. This property was tremendously improved by adding a 2.5 wt % of styrene to the formulation. The resulting latex had a 32% gel fraction and a higher sol $\bar{M}_w$. Comparison with the results obtained with 0.06 wt % of CTA showed that the good resistance to shear was mostly due to the lower gel fraction. Almost no gel was found when the styrene content was increased to 10 wt %. Nevertheless, this latex showed an appreciable shear resistance that was due to the high $\bar{M}_w$ (the latex prepared with 0.15 wt % of CTA that contained no gel and had a low $\bar{M}_w$ presented a poor shear resistance). These results demonstrated that the amount of gel of a polymer was critical to determine its resistance to shear.

A similar trend was observed for the resistance to peel of the latexes prepared with different amounts of styrene. The resistance to peel increases from 6.0 to 26 N/100 nm when the fraction of gel increases from 0 to 32%. It means that the gel decreases the free movement of polymer molecules and thereby increases the cohesive strength of the latex in a first stage. It is worth noting that latexes without gel polymer but having different molecular weights, namely those prepared with 10 wt % styrene in this work and 0,15 wt % CTA in ref 17, presented a difference in the resistance to peel. Thus, resistance to peel decreased from 11 to 6 N/100 nm, whereas resistance to shear increased from 45 to 1051 s, for the latexes prepared with 0.15 wt % of CTA and 10 wt % of styrene, respectively. Nevertheless, further increasing gel polymer does not mean an increase in the resistance to peel. This can be seen for the latex prepared without styrene, where the resistance to peel lowered to 16.9 N/100 nm. The reason being that the network is so rigid that it does not allow any mobility of the polymer chains.

Effect of Feeding Time. Two additional experiments were carried out using a longer feeding time (lower feed flow rate) for the experiments with 5 and 10 wt % of styrene. Table 3 shows the formulations used. These new experiments aimed to investigate the effect of the feeding time on gel content, sol molecular weight distribution and branching level in the copolymerization of *n*-BA with small amounts of styrene.

Figure 9 shows the evolution of the instantaneous conversion for runs 4−7. It can be seen that the longer the monomer feeding time the higher the instantaneous

Table 7. Comparison between the Experimental and Predicted Level of Branches, Weight-Average Molecular Weight, and Gel Fraction for the Final Latexes Produced in the Experiments with 3 and 6 h of Feeding Time Using 5 and 10 wt % of Styrene in the Recipe

	experimental results			model predictions		
process variables	level of branches (%)	gel fraction (%)	$\bar{M}_w$	level of branches (%)	gel fraction (%)	$\bar{M}_w$
5 wt % styrene						
run 4 (3 h)	1.3	12	1.26×10^6	1.2	25.4	1.23×10^6
run 6 (6 h)	1.8	20	0.87×10^6	1.8	31	1.10×10^6
10 wt % styrene						
run 5 (3 h)	0.9	1	1.58×10^6	0.89	16.0	1.10×10^6
run 7 (6 h)	1.0	1	1.16×10^6	1.22	17.9	1.04×10^6

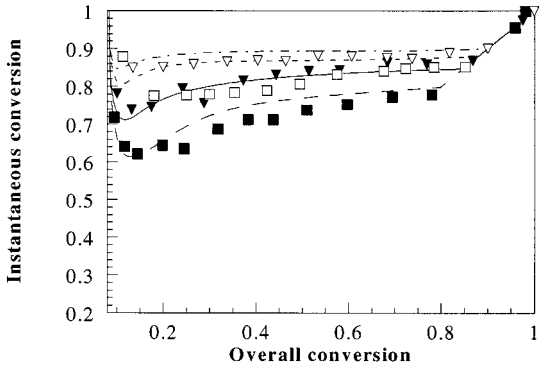

Figure 9. Experimental and predicted instantaneous conversion for runs 4, 5, 6, and 7 where the feeding time was varied. Legend: feeding time = 3 h, (▼, —) 5 wt % and (■, — —) 10 wt %; feeding time = 6 h, (▽, - -•- -) 5 wt % and (□, - -) 10 wt %.

conversion. Model predictions are in fair agreement with the experimental data.

Table 7 presents the experimental and model predictions for the final contents of gel, level of branches and average molecular weights for the experiments with 5 and 10 wt % of styrene in the recipe carried out using monomer feeding times of 3 and 6 h. For the experiments carried out with 5 wt % of styrene both the percentage of branches and the gel content increased but $\bar{M}_w$ decreased with increasing feeding time. Model predictions are in good agreement with the experimental data. The model shows that increasing feeding time led to the reduction of the concentration of monomer in the polymer particles (Figure 9). This caused an increase of the level of branches due to the higher probability for backbiting. In addition, the increase of polymer concentration in the particles enhanced the probability of intermolecular transfer to polymer and hence the formation of gel, which in turn led to a decrease of the molecular weight of the sol. The mathematical model predicts that the amount of short chain branches (intramolecular transfer or backbiting) was 2 orders of magnitude larger than the long chain branches (intermolecular transfer). For the experiments with 10 wt % of styrene no significant effect of the feeding time on branching level and gel content was observed. It is worth pointing out that the sensitivity of the characterization techniques to measure both gel contents and level branches is limited in this region. Table 7 shows that the molecular weights decreased by increasing the feeding time.

Conclusions

The kinetics of the seeded semicontinuous emulsion copolymerization of *n*-BA/S and the structural properties of the resulting copolymers have been investigated. It was found that an increase of the amount of styrene yielded to a decrease of the instantaneous conversion and the polymerization rate. Also, the larger the amount of styrene, the smaller the gel content. It is worth pointing out that the addition of 10% of styrene was sufficient to practically avoid the formation of gel. In contrast, the average molecular weights of the sol were only slightly affected; the increase of the amount of styrene resulted in a slight increase of the molecular weights.

These results have a significant impact on the adhesive properties of the latexes. Thus, we found that a balance between amount of gel and high $\bar{M}_w$ is the best choice to enhance resistance to peel and shear simultaneously.

In addition, a mathematical model for the calculation of kinetics, branching frequency, sol molecular weight distribution, and gel fraction was developed. The model explained with accuracy the results obtained experimentally for the kinetics, and latex properties (as gel, sol molecular weight, and branching level) when small amounts of styrene where included in the formulation. This will allow to tailor formulations and feed policies to produce copolymer latexes with the desired structural properties to be used as pressure sensitive adhesives.

Appendix I. Mathematical Model

Reactant Balances. Evolution of the Kinetics. The material balances of reactants for a semicontinuous process are

$$\frac{di}{dt} = F_i \pm R_i \tag{I-1}$$

where i is the total number of moles of compound i in the reactor, F_i the molar feed rate of compound i and R_i its rate of appearance or disappearance by reaction.

The rate of decomposition of a water-soluble initiator can be expressed as

$$R_I = k_I I_2 \tag{I-2}$$

The rate of monomer consumption can be expressed as

$$R_p = \bar{k}_p [M]_p \frac{\bar{n} N_p}{N_A} \tag{I-3}$$

The monomer concentration in the polymer particles, $[M]_p$, is calculated using the partition equilibrium equations and the monomer material balance by means of an iterative algorithm.[40,41]

The model was developed for the seeded semibatch copolymerization of S/*n*-BA. As shown in Figure 3, N_p was almost constant throughout the polymerizations and it was not affected by the operational variables (styrene ratio and monomer feed flow rate). Thus, and

for the sake of simplicity a polynomial fitting of the evolution of the experimental particle diameter was used to account for the total number of particles.

To integrate the monomer balance the evolution of $\bar{n}$ during the reaction is required. This was done by using the approach proposed by Ugelstad and Hansen[31] (eq I-4) combined with the radical balance in the aqueous phase (eq I-5).

$$\bar{n} = \cfrac{a^2/8}{m + \cfrac{a^2/4}{m + 1 + \cfrac{a^2/4}{m + 2 + \ldots}}}$$

$$\text{where} \quad m = \frac{k_d \nu_p N_A}{k_t} \quad \text{and} \quad a^2 = 8 k_a [R]_w \tag{I-4}$$

$$\frac{d[R]_w}{dt} = 0 = 2 f k_I I_2 N_A + k_d \bar{n} N_p - k_a [R]_w N_p - 2 k_{tw} [R]_w^2 N_A \tag{I-5}$$

The instantaneous conversion is given by

$$X_{inst} = \frac{M_t - M + M_{seed}}{M_t + M_{seed}} \tag{I-6}$$

where

$$M_t = M_o + \int_0^t F_M \, dt \tag{I-7}$$

Branching Frequency. The balance of overall branching points including short and long chain branches is

$$\frac{dB}{dt} = \bar{k}_{fp1} [Q_1]_p Y_{BA} \bar{n} N_p + \bar{k}_{fp2} Y_{BA,inst} \bar{n} N_p \tag{I-8}$$

The frequency of branching is calculated as the ratio between branching points and the monomeric units polymerized, Q_1 as

$$\nu_B = B/Q_1 \tag{I-9}$$

where Q_1 is given by

$$Q_1 = (M_o + \int_0^t F_M \, dt - M) N_A \tag{I-10}$$

Molecular Weights of Soluble Fraction ($\bar{M}_{n,sol}$, $\bar{M}_{w,sol}$) and Gel Fraction. To describe the sol MWD in detail, a refined numerical fractionation approach was used.[25] In addition, the accurate calculation of the polymer structure requires a good description of the sol MWD and to account for the compartmentalization of radicals. For these reasons, compartmentalization was accounted for by means of the partial distinction approach.[26] Hence the free radical population is divided into "short" (q) and "long" (p) radicals. For the current system it is considered that linear radicals are "short", whereas branched polymers are "long". Using this distribution, the number ($\bar{M}_{n,sol}$) and weight ($\bar{M}_{w,sol}$) average molecular weights of the sol fraction are as follows:

$$\bar{M}_{n,sol} = \frac{\sum_{n=0}^{n_c} Q_1(n) + \sum_{n=0}^{n_c} \sum_{i=1}^{m} p_1^i(n) + q_1^i(n)}{\sum_{n=0}^{n_c} Q_0(n) + \sum_{n=0}^{n_c} \sum_{i=1}^{m} p_0^i(n) + q_0^i(n)} P_m \tag{I-11}$$

$$\bar{M}_{w,sol} = \frac{\sum_{n=0}^{n_c} Q_2(n) + \sum_{n=0}^{n_c} \sum_{i=1}^{m} p_2^i(n) + q_2^i(n)}{\sum_{n=0}^{n_c} Q_1(n) + \sum_{n=0}^{n_c} \sum_{i=1}^{m} p_1^i(n) + q_1^i(n)} P_m \tag{I-12}$$

The fraction of gel was calculated by the difference between the total amount of polymerized monomer units and the monomer units in the polymer chains generations up to n_c:

$$\text{Gel} = \frac{Q_1 + \sum_{i=1}^{m} (p_1^i + q_1^i) - (\sum_{n=0}^{n_c} Q_1(n) + \sum_{n=0}^{n_c} \sum_{i=1}^{m} p_1^i(n) + q_1^i(n))}{Q_1 + \sum_{i=1}^{m} (p_1^i + q_1^i)} \tag{I-13}$$

n_c is the last generation considered in the computation of the sol MWD. The calculation of the moments of chain length distributions of both dead and active polymer is given in Appendix II. Gel is considered to be all of the polymer having a molecular weight larger than 7×10^6.

Appendix II. Moments of the Chain Length Distributions of Dead and Active Polymer

The balances for the kth-order moments of the overall chain length distribution of the dead polymer in generation n, ($Q_k(n)$), can be expressed as the sum of the contributions of each of the processes, s, leading to the formation of dead polymer in the particles containing different number of radicals, i.

$$\frac{dQ_k(n)}{dt} = \sum_s \sum_{i=1}^{m} \frac{dQ_{k,s}^i(n)}{dt} \tag{II-1}$$

The kth-order moments of the chain length distribution of dead polymer produced by the different mechanisms are as follows.

Chain transfer to monomer

$$\frac{dQ_{k,f}^i(n)}{dt} = \bar{k}_{fm} [M]_p (p_k^i(n) + q_k^i(n)) \tag{II-2}$$

Chain transfer to polymer

$$\frac{dQ_{k,fp}^i(n)}{dt} = \bar{k}_{fp1} [Q_1] Y_{BA} (p_k^i(n) + q_k^i(n)) \tag{II-3}$$

Termination by combination

$$\frac{dQ_{kctc}{}^{i}(n)}{dt} = c_{tc}\sum_{\substack{j=0\\k=i-j}}^{i}\frac{1}{N_{i,j,k}}\left\{\left(\frac{j-1}{j}p_0{}^{i}(n)^2\mu_k{}^{i}(p_n,p_n) + 2p_0{}^{i}(n)q_0{}^{i}(n)\mu_k{}^{i}(p_n,q_n) + \frac{k-1}{k}q_0{}^{i}(n)^2\mu_k{}^{i}(q_n,q_n)\right)\delta_{n=0} + \sum_{\substack{h=0\\l=n-h}}^{n}\left(\frac{j-1}{j}p_0{}^{i}(h)p_0{}^{i}(l)\mu_k{}^{i}(p_h,p_l) + 2p_0{}^{i}(h)q_0{}^{i}(l)\mu_k{}^{i}(p_h,q_l)\right)\delta_{0<n\le n_e} + \sum_{h=0}^{n_e+1}\sum_{l=n_e+1-h}^{n_e+1}\left(\frac{j-1}{j}p_0{}^{i}(h)p_0{}^{i}(l)\mu_k{}^{i}(p_h,p_l) + 2p_0{}^{i}(h)q_0{}^{i}(l)\mu_k{}^{i}(p_h,q_l)\right)\delta_{n=n_e+1} - \left(\frac{j-1}{j}p_0{}^{i}(n)^2\mu_k{}^{i}(p_n,p_n)\right)\delta_{n=n_e+1} + \left(\frac{j-1}{j}p_0{}^{i}(n-1)^2\mu_k{}^{i}(p_{n-1},p_{n-1})\right)\delta_{n_e+1\le n\le n_c} + 2p_0{}^{i}(n)\sum_{h=0}^{n}\left(\frac{j-1}{j}p_0{}^{i}(h)\mu_k{}^{i}(p_h,p_n) + 2q_0{}^{i}(h)\mu_k{}^{i}(p_h,q_n)\right)\delta_{n_e+1\le n\le n_c}\right\} \quad \text{(II-4)}$$

$\mu_k{}^{i}(p_h,q_l)$, the instantaneous kth-order moment of inactive polymer produced through the combination of a radical $p^i(h)$ and a radical $q^i(l)$ are expressed as[42]

$$\mu_0{}^{i}(p_h,q_l) = 1 \quad \text{(II-5)}$$

$$\mu_1{}^{i}(p_h,q_l) = \frac{p_1{}^{i}(h)}{p_0{}^{i}(h)} + \frac{q_1{}^{i}(l)}{q_0{}^{i}(l)} \quad \text{(II-6)}$$

$$\mu_2{}^{i}(p_h,q_l) = \frac{p_2{}^{i}(h)}{p_0{}^{i}(h)} + \frac{q_2{}^{i}(l)}{q_0{}^{i}(l)} + \left(\frac{p_1{}^{i}(h)}{p_0{}^{i}(h)}\right)^2 + \left(\frac{q_1{}^{i}(l)}{q_0{}^{i}(l)}\right)^2 \quad \text{(II-7)}$$

$N_{i,j,k}$ represents the number of particles containing i radicals, j (branched) "long" radicals, and k (linear) "short" radicals and can be calculated as

$$\frac{dN_{i,j,k}}{dt} = 0 = k_a[R]_w N_{i-1}\delta_{k=1} + \bar{k}_{fm}[M]_p(j+1)N_{i,j+1,k-1}\delta_{2\le k\le i-1} + \bar{k}_{fp1}[Q_1]Y_{BA}(k+1)N_{i,j-1,k+1} - (k_a[R]_w + \bar{k}_{fm}[M]_p j + ci(i-1) + k_d k + \bar{k}_{fp1}[Q_1]Y_{BA}k)N_{i,j,k} \quad \text{for } j \ne i \quad \text{(II-8)}$$

$$N_{i,i,0} = N_i - \sum_{k=1}^{i-1}N_{i,j,k} \quad \text{(II-9)}$$

The zeroth-, first-, and second-order moments of length distribution of radicals q (belonging to the linear generation) are expressed as

$$\frac{dq_0{}^{i}(0)}{dt} = 0 = k_a[R]_w(N_{i-1} - q_0{}^{i}(0)) - k_d(iN_i + (i-1)q_0{}^{i}(0)) + \bar{k}_{fm}[M]_p(iN_i - q_0{}^{i}(0)) - \bar{k}_{fp1}[Q_1]Y_{BA}q_0{}^{i}(0) - ci(i-1)q_0{}^{i}(0) \quad \text{(II-10)}$$

$$\frac{dq_1{}^{i}(0)}{dt} = 0 = k_a[R]_w(N_{i-1} - q_1{}^{i}(0)) - k_d(iN_i + (i-1)q_1{}^{i}(0)) + \bar{k}_{fm}[M]_p(iN_i - q_1{}^{i}(0)) - \bar{k}_{fp1}[Q_1]Y_{BA}q_1{}^{i}(0) - ci(i-1)q_1{}^{i}(0) + \bar{k}_p[M]_p q_0{}^{i}(0) \quad \text{(II-11)}$$

$$\frac{dq_2{}^{i}(0)}{dt} = 0 = k_a[R]_w(N_{i-1} - q_2{}^{i}(0)) - k_d(iN_i + (i-1)q_2{}^{i}(0)) + \bar{k}_{fm}[M]_p(iN_i - q_2{}^{i}(0)) - \bar{k}_{fp1}[Q_1]Y_{BA}q_2{}^{i}(0) - ci(i-1)q_2{}^{i}(0) + \bar{k}_p[M]_p(2q_1{}^{i}(0) + q_0{}^{i}(0)) \quad \text{(II-12)}$$

The zeroth-, first-, and second-order moments of length distribution of radicals p (belonging to a general branched or linear generation) are expressed as

$$\frac{dp_0{}^{i}(n)}{dt} = 0 = k_a[R]_w\left((p_0{}^{i-1}(n) + q_0{}^{i-1}(n)) + \frac{i}{i+1}(p_0{}^{i+1}(n) + q_0{}^{i+1}(n))\delta_{j=m-1} - p_0{}^{i}(n)\right) + k_d(i(p_0{}^{i+1}(n) + q_0{}^{i+1}(n)) - (i-1)p_0{}^{i}(n)) - \bar{k}_{fm}[M]_p p_0{}^{i}(n) + c(i(i+1)(p_0{}^{i+2}(n) + q_0{}^{i+2}(n)) - i(i-1)p_0{}^{i}(n)) + \bar{k}_{fp1}([Q_1(n-1)]iN_i\delta_{n\le n_e+1} + [Q_1(n)]iN_i\delta_{n\ge n_e+1} - [Q_1]p_0{}^{i}(n))Y_{BA} \quad \text{(II-13)}$$

$$\frac{dp_1{}^{i}(n)}{dt} = 0 = k_a[R]_w\left((p_1{}^{i-1}(n) + q_1{}^{i-1}(n)) + \frac{i}{i+1}(p_1{}^{i+1}(n) + q_1{}^{i+1}(n))\delta_{j=m-1} - p_1{}^{i}(n)\right) + k_d(i(p_1{}^{i+1}(n) + q_1{}^{i+1}(n)) - (i-1)p_1{}^{i}(n)) - \bar{k}_{fm}[M]_p p_1{}^{i}(n) + c(i(i+1)(p_1{}^{i+2}(n) + q_1{}^{i+2}(n)) - i(i-1)p_1{}^{i}(n)) + \bar{k}_p[M]_p p_0{}^{i}(n) + \bar{k}_{fp1}([Q_2(n-1)]iN_i\delta_{n\le n_e+1} + [Q_2(n)]iN_i\delta_{n\ge n_e+1} - [Q_1]p_1{}^{i}(n))Y_{BA} \quad \text{(II-14)}$$

$$\frac{dp_2{}^{i}(n)}{dt} = 0 = k_a[R]_w\left((p_2{}^{i-1}(n) + q_2{}^{i-1}(n)) + \frac{i}{i+1}(p_2{}^{i+1}(n) + q_2{}^{i+1}(n))\delta_{j=m-1} - p_2{}^{i}(n)\right) + k_d(i(p_2{}^{i+1}(n) + q_2{}^{i+1}(n)) - (i-1)p_2{}^{i}(n)) - \bar{k}_{fm}[M]_p p_2{}^{i}(n) + c(i(i+1)(p_2{}^{i+2}(n) + q_2{}^{i+2}(n)) - i(i-1)p_2{}^{i}(n)) + \bar{k}_p[M]_p(2p_1{}^{i}(n) + p_0{}^{i}(n)) + \bar{k}_{fp1}([Q_3(n-1)]iN_i\delta_{n\le n_e+1} + [Q_3(n)]iN_i\delta_{n\ge n_e+1} - [Q_1]p_2{}^{i}(n))Y_{BA} \quad \text{(II-15)}$$

Notice that a closure problem appears to solve the active and inactive chains balances, because every moment

depends on the next higher. Therefore, following the Saidel and Katz[43] approximation, the third moment was calculated as

$$Q_3(n) = \frac{2Q_2^{\,2}(n)}{Q_1(n)} - \frac{Q_2(n)Q_1(n)}{Q_0(n)} \qquad \text{(II-16)}$$

The zeroth order moment of the overall distributions of radicals in particles containing i radicals, p^i and q^i are

$$\bar{p}_0^{\,i} = \sum_{j=1}^{i} jN_{i,j,k} \qquad \text{(II-17)}$$

$$\bar{q}_0^{\,i} = \sum_{k=1}^{i} kN_{i,j,k} \qquad \text{(II-18)}$$

Acknowledgment. The support in analyzing the samples by ^{13}C NMR by Professor Juan M. Alberdi is greatly appreciated. The support of Matías Vicente in analyzing the adhesive properties is also greatly appreciated.

References and Notes

(1) Odian, G. In *Principles of Polymerization*, 3rd ed.; John Wiley & Sons Inc.: New York, 1991; p 453.
(2) Leiza, J. R.; Asua, J. M. In *Polymeric Dispersions: Principles and Applications*; Asua, J. M., Ed.; NATO ASI Series; Kluwer Academic Publishers: 1997; Vol E−335, p 363.
(3) López de Arbina, L.; Barandiaran, M. J.; Gugliotta, L. M.; Asua, J. M. *Polymer* **1997**, *38* (1), 143.
(4) van Doremaele, G. H. J. Ph.D. Dissertation, Eindhoven University of Technology, 1991.
(5) de la Cal, J. C.; Adams, M. E.; Asua, J. M. *Makromol. Chem., Macromol. Symp.* **1990**, *35/36*, 23.
(6) Cruz, M. A.; Palacios, J.; Garcia, A.; Ruiz, L. M.; Rios, L. *Makromol. Chem. Suppl.* **1985**, *10/11*, 87−103.
(7) Chrástová, V.; Citovicky, P.; Bartus, J. *Pure Appl. Chem.* **1994**, *A31*, 835−846.
(8) Fernandez-Garcia, M.; Fernandez-Sanz, M.; Madruga, E. L.; Fernandez-Monreal, C. *Makromol. Chem. Phys.* **1999**, *200*, 199−205.
(9) Ziaee, F.; Nekoomanesh, M. *Polymer* **1998**, *39* (1), 203.
(10) Dubé, M.; Penlidis, A.; O'Driscoll, K. F. *Chem. Eng. Sci.* **1990**, *45*, 2785.
(11) Chrástová, V.; Bartus, J.; Zarras, P. *Pure Appl. Chem.* **1996**, *A33*, 13.
(12) Yang, H.-Y.; Yang, C.-H. *J. Appl. Polym. Sci.* **1998**, *69*, 551.
(13) Charmot, D. In *Polymeric Dispersions: Principles and Applications*; Asua, J. M., Ed.; NATO ASI Series; Kluwer Academic Publishers: 1997; Vol. E−335, p 79.
(14) Plessis, C.; Arzamendi, G.; Leiza, J. R.; Schoonbrood, H. A. S.; Charmot, D.; Asua, J. M. *Macromolecules* **2000**, *33*, 4.
(15) Plessis, C.; Arzamendi, G.; Leiza, J. R.; Schoonbrood, H. A. S.; Charmot, D.; Asua, J. M. *Macromolecules* **2000**, *33*, 5041.
(16) Plessis, C.; Arzamendi, G.; Leiza, J. R.; Schoonbrood, H. A. S.; Charmot, D.; Asua, J. M. *Ind. Eng. Chem. Res.* **2000** (in press).
(17) Plessis, C.; Arzamendi, G.; Leiza, J. R.; Alberdi, J. M.; Schoonbrood, H. A. S.; Charmot, D.; Asua, J. M. *J. Polym. Sci., Part A: Polym. Chem.* **2001**, *39* (7), 1006.
(18) Cohen-Addad, J. P.; Bogonuk, C.; Granier, V. *Macromolecules* **1994**, *27*, 5032.
(19) Ahmad, N. M.; Heatley, F.; Lovell, P. A. *Macromolecules* **1998**, *31*, 2822.
(20) Lovell, P. A.; Shah, T. H.; Heatley, F. *Polym. Commun.* **1991**, *32*, 4, 98.
(21) Phaen, Q. T.; Petiand, R.; Waton, H.; Llauro-Darricades, M. F. In *Proton and Carbon NMR Spectra of Polymers*; Penton Press: London, 1991.
(22) *Standard methods of Testing Pressure-Sensitive tapes*; Pressure Sensitive Tape Council: Glenview, IL, 1976.
(23) Teymour, F.; Campbell, J. D. *DECHEMA Monogr.* **1992** *127*.
(24) Teymour, F. Campbell, J.D. *Macromolecules* **1994**, *27*, 2460.
(25) Arzamendi, G.; Asua, J. M. *Macromolecules* **1995**, *28*, 7479.
(26) Arzamendi, G.; Sayer, C.; Zoco, N.; Asua, J. M. *Polym. React. Eng.* **1998**, *6* (3&4), 193.
(27) Forcada, J.; Asua, J. M. *J. Polym. Sci.: Polym. Chem. Ed.* **1985**, *23*, 1955.
(28) Friis, N.; Hamielec, A. E. *J. Polym. Sci.: Polym. Chem. Ed.* **1974**, *12*, 251.
(29) Friis, N.; Hamielec, A. E. In *Emulsion Polymerization*; Piirma, I., Berge, A., Eds.; Academic Press: New York, 1982.
(30) Lee, C.-F.; Chiu, W−E.; Chern, Y.-C. *J. Appl. Polym. Sci.* **1995**, *57*, 591.
(31) Ugelstad, J.; Hansen, F. K. *Rubber Chem. Technol.* **1976**, *49*, 536−609.
(32) Asua, J. M.; Sudol, E. D.; El-Aasser, M. S. *J. Polym. Sci., Polym. Chem. Ed.* **1989**, *27*, 1903.
(33) Nelder, J. A.; Mead, R. *Comput. J.* **1964**, *7*, 308.
(34) Buback, M.; Kuchta, F.-D. *Macromol. Chem. Phys.* **1997**, *198*, 1455.
(35) Elias, H. G. *Macromolecules*; Plenum Press: New York, 1984; p 700.
(36) Lopez de Arbina, L. Ph.D. Dissertation, University of Basque Country, Donostia-San Sebastián, 1996.
(37) Maeder, S.; Gilbert, R. G. *Macromolecules* **1998**, *31*, 4410.
(38) Bandrup, J.; Immergut, E. H. In *Polymer Handbook*, 3rd Ed.; Wiley-Interscience publication, John Wiley and Sons: New York, 1989.
(39) Satas, D. *Handbook of Pressure Sensitive Adhesive Technology*; Van Nostrand Reinhold: New York, 1989.
(40) Omi, S.; Kushibiki, K.; Negishi, M.; Iso, M. *Zairyo Gijutzu* **1985**, *3*, 426.
(41) Urretabizkaia, A.; Arzamendi, G.; Asua, J. M. *Chem. Eng. Sci.* **1992**, *47*, 2579.
(42) Villermaux, J. L.; Blavier, G. *Chem. Eng. Sci.* **1984**, *39*, 87−99.
(43) Saidel, G. M.; Katz, S. *J. Polym. Sci. Polym. Phys.* **1968**, *6*, 1149.

MA0020382